



**HAL**  
open science

## ROUGH NICKEL SELECTIVE COATINGS OBTAINED BY ELECTROCHEMICAL PROCESSES

J. Amblard, M. Froelicher, G. Blondeau, J. Lafait, J. Behaghel, R. Herrera

► **To cite this version:**

J. Amblard, M. Froelicher, G. Blondeau, J. Lafait, J. Behaghel, et al.. ROUGH NICKEL SELECTIVE COATINGS OBTAINED BY ELECTROCHEMICAL PROCESSES. Journal de Physique Colloques, 1981, 42 (C1), pp.C1-147-C1-160. 10.1051/jphyscol:1981110 . jpa-00220660

**HAL Id: jpa-00220660**

**<https://hal.science/jpa-00220660>**

Submitted on 4 Feb 2008

**HAL** is a multi-disciplinary open access archive for the deposit and dissemination of scientific research documents, whether they are published or not. The documents may come from teaching and research institutions in France or abroad, or from public or private research centers.

L'archive ouverte pluridisciplinaire **HAL**, est destinée au dépôt et à la diffusion de documents scientifiques de niveau recherche, publiés ou non, émanant des établissements d'enseignement et de recherche français ou étrangers, des laboratoires publics ou privés.

## ROUGH NICKEL SELECTIVE COATINGS OBTAINED BY ELECTROCHEMICAL PROCESSES.

J. Amblard (\*), M. Froelicher (\*), G. Blondeau (\*), J. Lafait (\*\*),  
J.M. Behaghel (\*\*) and R. Herrera (\*\*)

(\*) Groupe de Recherche n° 4 du C.N.R.S. "Physique des Liquides et Electrochimie"  
(\*\*) et Laboratoire d'Optique des Solides, Université Pierre et Marie Curie, 4  
place Jussieu, 75230 Paris Cedex 05, France.

Résumé.- On montre comment optimiser les paramètres électrochimiques pour:

- 1) obtenir sur un substrat métallique un dépôt cathodique de Ni de rugosité bien contrôlée et reproductible
- 2) améliorer l'absorptivité solaire de ce dépôt rugueux grâce à une oxydation anodique superficielle ultérieure.

Un modèle électromagnétique rend compte de façon satisfaisante des propriétés optiques des couches Ni + NiO ainsi obtenues.

Abstract.- We show below how to optimize electrochemical parameters in order to :

- 1) plate on a metallic substrate a Ni cathodic deposit with a well defined, reproducible roughness
- 2) improve the solar absorptance of this rough deposit thanks to a subsequent anodic oxidization.

An electromagnetic model accounts fairly well for the optical properties of the Ni + NiO layers thus obtained.

1. Introduction.- One among the simplest ideas in order to create a selective reflection-absorption filter, according to Tabor's definition /1/ is to start from a metal, which is a good reflector for long wave radiation, and blacken it by some appropriate device. The first requirement for such a device is to be inexpensive, which explains the common use of electroplating or chemical conversion in most processes available nowadays. But such processes, which have been often developed empirically, are very sensitive to any variation in the preparation procedure and hence give hardly reproducible results. Moreover, as the structure of the usually very thin superficial layer responsible for solar absorption is complex, it is too much sensitive to thermal cycling, UV irradiation and air corrosion. Hence further progress has to be made towards the realization of reproducible, stable and structurally well-defined selective solar absorbers.

The aim of our paper is to show how, starting from Watts nickel electrodeposits whose structure has been fully described during the last decade, it is possible to optimize the deposition parameters in order to obtain a reproducible, adequate roughness and then good solar selective properties. The optimal selectivity is achieved through the use

of a mere Ni chloride bath in well-defined plating conditions and it may be characterized by the best solar absorptance ( $\alpha \approx 0.8$ ) and a typical emittance  $\varepsilon \approx 0.2$  at 200°C. Such an absorptance is then further improved (up to  $\alpha \approx 0.95$ ) thanks to another electrochemical process, namely an anodic oxidization in a concentrated sulfuric acid medium, which leads to the formation of a thin NiO superficial layer responsible for an additional destructive interference effect in the very range of maximal solar intensity. One may expect furthermore from that NiO layer a better resistance against thermal oxidization and air corrosion.

2. Cathodic process.- We shall describe first how to obtain dendritic surfaces of electrodeposited Ni by a proper choice of plating conditions and then characterize their optical properties from which are computed both  $\alpha$  and  $\varepsilon$ .

2.1. Choice of electroplating conditions.- We know from a 10-year experience that physical properties of electrodeposits strongly depend on plating conditions. This is particularly true for nickel, whose deposits offer a wide variety of appearances according to the composition of the bath they come from. Thus we can readily eliminate the plating solutions containing organic additives (in as much as they very often lead to mirror-bright deposits) and restrict the discussion to a conventional organic-free Watts bath which is well known for giving duller deposits /2/. But, even under that restriction, the problem is far from being solved. The way rough Ni electrodeposits intercept the visible light still depends on every other plating condition such as bath temperature and pH, cathodic potential and current density, deposit thickness, etc ...

A major key of understanding such a dependency is to consider a fundamental structural property of Ni electrodeposits, namely their texture. Once a deposit is thick enough to be free from the epitaxial influence of the substrate (which means a thickness of several microns on a mechanically-polished substrate /3/), it appears to be made of fiberlike crystallites which grow along a definite crystallographic direction  $[h k l]$ . On the nature of  $[h k l]$  depend not only the physical properties of the deposit, among which are its roughness and reflectivity, but even the very mode of growth which engenders it /4/.

Figure 1 shows the various textures encountered in thick Ni deposits from a Watts bath of a given composition ( $\text{NiSO}_4 \cdot 7 \text{H}_2\text{O} = 300 \text{ g/l}$  ;  $\text{NiCl}_2 \cdot 6 \text{H}_2\text{O} = 35 \text{ g/l}$  ;  $\text{H}_3\text{BO}_3 = 40 \text{ g/l}$ ), operated at 50°C for different pH and current densities. Further details are given elsewhere /5/. Additional structural data have been obtained from transmission /6/ and scanning /7/ electron microscopy observations. All of these deposits are made of fibers, the mean diameter of which is typically one micron. They essentially differ by the kind of the crystallographic facets which delimit

their superficial morphology : the steepest slopes are encountered in  $\langle 110 \rangle$  deposits which are therefore the dullest. Hence we must expect the best solar absorptance for Ni electrodeposits exhibiting a  $\langle 110 \rangle$  texture.

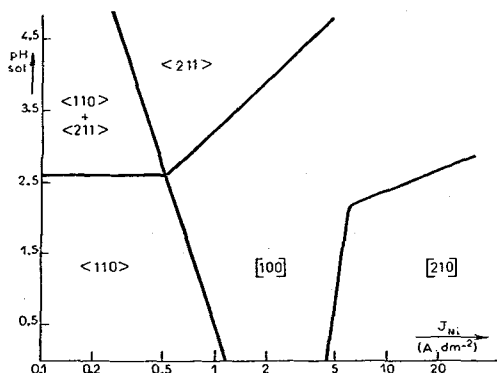


Fig.1.- Stability diagram for the various textures encountered in thick Ni electrodeposits obtained from an organic-free Watts bath at 50°C, against Ni partial current density and solution pH. Each texture corresponds to a definite mode of growth and thus to a definite superficial morphology.

The structure of each crystallite of a  $\langle 110 \rangle$  deposit is somewhat peculiar and thus is worth being described in more detail : each fiber has a prismatic form with an overall fivefold symmetry. Of course it is not a true crystallographic symmetry, as can be seen from the microdiffraction of figure 2b : the five sectors a crystallite is made of (Fig. 2a) are separated by vertical twin planes and they have a common  $\langle 110 \rangle$  axis which has been proved to play a major role in the growth of the  $\langle 110 \rangle$  fiber /6,7/.

When the mean growth rate is low, which is the case for  $\langle 110 \rangle$  Ni deposits from a Watts bath since the maximum growth rate for  $\langle 110 \rangle$  is about 10 Å per second, the tip of the fibers is delimited by  $(111)$  planes which are then inclined at an angle of 35° towards the substrate (see the carbon replica of Fig. 2c). Steeper slopes may be expected from higher growth rates, when the  $\langle 110 \rangle$  fiber axis grows fast enough not to permit  $(111)$  equilibrium facets to be developed.

This is the reason why we turned to the use of Ni chloride baths which are known to enhance the stability of the  $\langle 110 \rangle$  texture and then of dark grey Ni electrodeposits /8/. All other plating conditions being kept constant, the whole effect of such a variation of the bath composition is a shift of the texture diagram of figure 1 towards higher current densities. Thus, it is possible, with a 300 g/l  $NiCl_2$ , 6  $H_2O$

bath for example, to obtain  $\langle 110 \rangle$  oriented Ni electrodeposits with 10-times faster growth rates. In these conditions the growth of  $\langle 110 \rangle$  fibers occurs mainly along the  $[110]$  axis with far more inclined facets, sometimes up to  $60-70^\circ$  in respect of the substrate as shown below in scanning electron micrographs of figures 4 and 7. From now on, we shall therefore only consider Ni electrodeposits obtained from such a chloride bath since their dendritic morphology seems capable of a high solar absorptance.

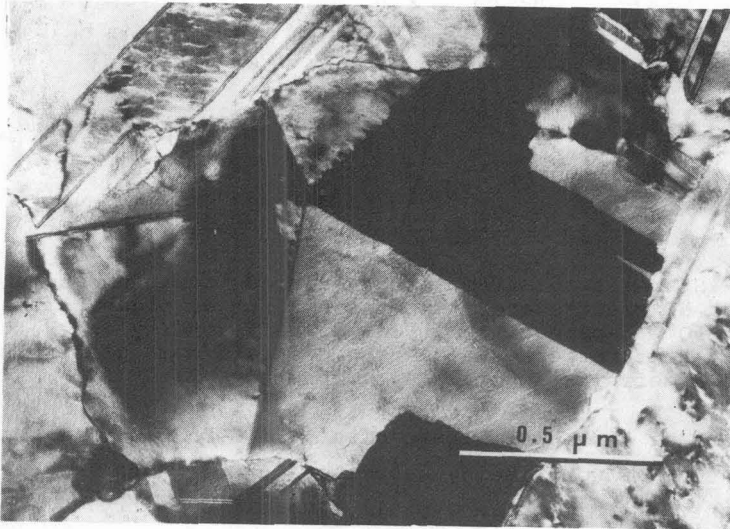


Fig.2a.-

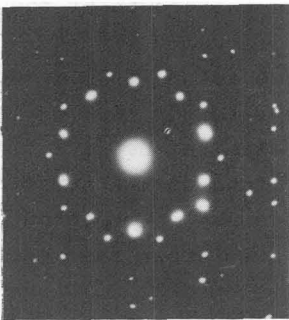


Fig.2b.-

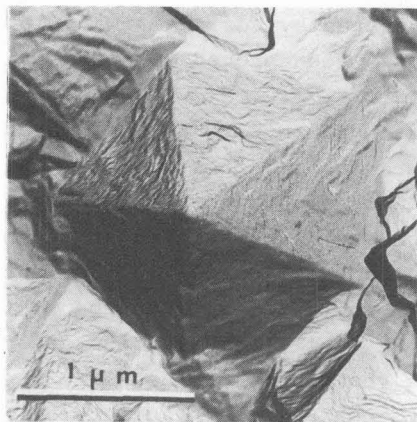


Fig.2c.-

Fig.2.- Detailed structural organization of a rough  $\langle 110 \rangle$  Ni deposit. Each fiber is made of five sectors (thin foil 2a) separated by vertical twin planes (microdiffraction 2b) with a common  $\langle 110 \rangle$  axis. The typical surface morphology is shown by the carbon replica 2c.

2.2. Optical properties of <1 1 0> Ni electrodeposits.- Since we now know the main structural features to be expected from our rough <1 1 0> deposits, it only remains to optimize the varying plating conditions -i.e. pH and current density- in order to obtain the highest solar absorptance  $\alpha$ . For that purpose we have undertaken a systematic study of the monochromatic hemispherical reflectance  $\rho(\lambda)$  of our samples, both in the visible and IR ranges, when varying the chloride solution pH from 0 up to 5 and the current density from 0.03 up to 3 A.dm<sup>-2</sup>. Details regarding optical techniques are given elsewhere /9,10/. For an opaque coating with zero transmittance, the conservation of energy can be written as :

$$\alpha(\lambda) = \epsilon(\lambda) = 1 - \rho(\lambda) \quad (1)$$

where  $\alpha(\lambda)$  and  $\epsilon(\lambda)$  are respectively the monochromatic absorptance and emittance at a given temperature. Then the best solar selective absorbers are those for which the absorptance  $\alpha(\lambda)$  is at a maximum -and hence  $\rho(\lambda)$  at a minimum- for the range of solar maximum intensity, i.e. for  $\lambda \sim 0.5 \mu\text{m}$ .

The optimum plating conditions, which lead to the lowest values of reflectance in the visible range, has been encountered for pH values between 1 and 2 and a current density of about 1 A.dm<sup>-2</sup>, which corresponds to a cathodic potential of -700 mV in respect of a calomel electrode saturated in KCl (SCE).

At these relatively low pH values the Ni deposition is accompanied by a strong hydrogen evolution which could be prejudicial to the metallic deposit. The evolved hydrogen must be then efficiently eliminated. Here the electrolyte stirring was ensured by rotation of the cathode at a constant angular velocity (1200 rev.min<sup>-1</sup>), but of course any other kind of efficient stirring is employable too.

The duration of the cathodic process must be great enough to allow for the typical superficial morphology to be developed, which means at least a two-hour deposition. Once the growth has reached the steady state conditions the deposit thickness is no longer critical and can be made several times greater without substantially affecting the roughness and hence the optical properties.

When operating with the aforementioned plating conditions, homogeneous Ni deposits are obtained with highly reproducible optical properties. Figure 3 gives a typical behaviour of their reflectance  $\rho(\lambda)$  as a function of wavelength between 0.3 and 13.5  $\mu\text{m}$ . On the same graph we attempted to account for such a behaviour thanks to the electromagnetic model developed by Beckmann (see more details in /11/) where intervene two gaussian distributions of roughnesses, each of them being characterized by

a mean quadratic amplitude  $\sigma$  and a spatial period  $T$ . Despite the fact that this theoretical model is only valid for smooth surfaces where the  $T/\sigma$  ratio is high, it still gives a fairly good simulation with the following computed values :

$\sigma_1 = 0.14 \mu\text{m}$  ;  $T_1 = 0.15 \mu\text{m}$ , for the low roughness which covers a surface area ratio of 0.7 and

$\sigma_2 = 0.60 \mu\text{m}$  ;  $T_2 = 0.54 \mu\text{m}$ , for the high roughness which covers the remaining area. When compared with the values estimated from scanning electron micrographs (Fig.4), we find a good concordance for the lowest roughness, while the highest is somewhat underestimated both in amplitude (by a factor of 2) and for the distance of correlation  $T_2$  (by a factor of 5).

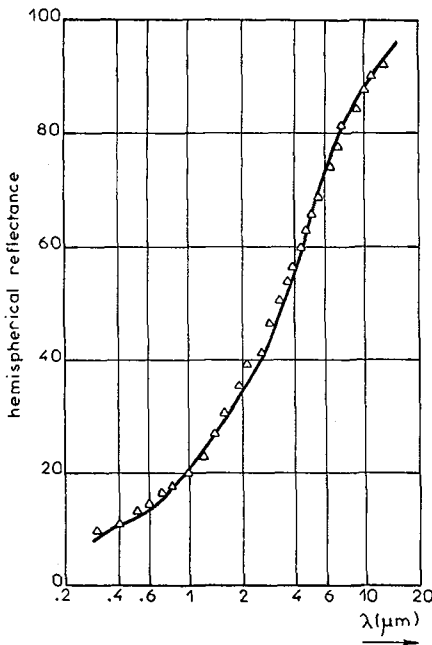


Fig.3.- Monochromatic hemispherical reflectance of a rough <1 1 0> Ni deposit obtained from a chloride bath at 50°C in optimized plating conditions.  $\Delta$  = optical measurements ; the solid line corresponds to computed data from Beckmann's model.

From the reflectance data of figure 3 and equations (1) it is now possible to evaluate the solar absorptance  $\alpha$  when using the solar spectral irradiance  $E^S(\lambda)$  as a weighting factor :

$$\alpha = \frac{\int_0^\infty \alpha(\lambda) E^S(\lambda) d\lambda}{\int_0^\infty E^S(\lambda) d\lambda} \tag{2}$$

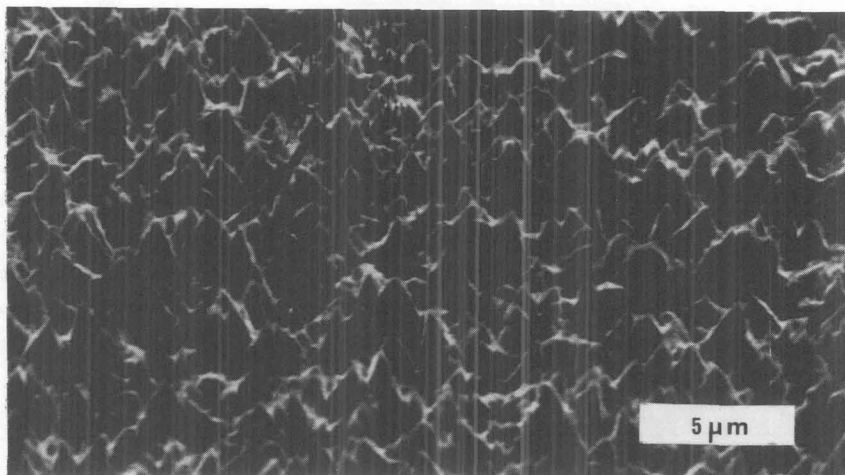


Fig.4a.-

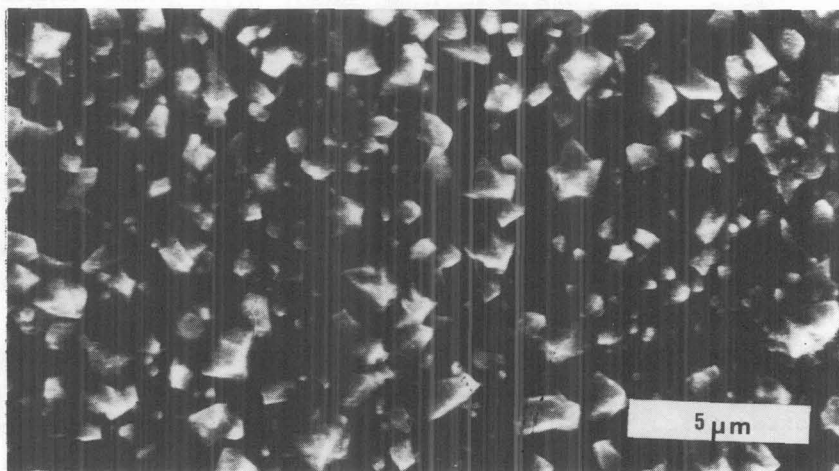


Fig.4b.-

Fig.4.- Scanning electron micrographs of the surface morphology of a rough  $\langle 110 \rangle$  Ni deposit. a/ grazing incidence, b/ normal incidence.

In the same way we calculate the total emittance  $\epsilon(T)$  at a given temperature when using the spectral emittance  $M^\circ(\lambda, T)$  of the black body at the same temperature as the weighting factor :

$$\epsilon(T) = \frac{\int_0^\infty \epsilon(\lambda) M^\circ(\lambda, T) d\lambda}{\int_0^\infty M^\circ(\lambda, T) d\lambda} \quad (3)$$

The results are given in table I where  $\alpha$  is successively computed for bright sun (air mass  $m = 1$ ), clouded sun (air mass  $m = 4$ ) and  $\epsilon$  for several temperatures up to 300°C. It can be seen that our best solar absorptance is very close to 0.8, which is a good performance if we keep in mind that roughness alone may account for it. It has often been stated that to produce higher selectivity requires the tandem action of at least two different physical processes /12/. Hence our dark grey Ni electrodeposits could yet be used as rough substrates (instead of Watts Ni) for "black Ni" or "black Cr" coatings /2/. But, in so far as these two processes are not thoroughly understood, we rather developed an anodic oxidization process which leads to comparable optical properties without markedly affecting the rough structure.

ABSORPTANCE $\alpha$		EMITTANCE $\epsilon(T)$			
bright sun air mass=1	clouded sun air mass =4	30°C	100°C	200°C	300°C
0.813	0.795	0.10	0.14	0.19	0.23

Table I.- Selectivity parameters for a rough  $\langle 110 \rangle$  Ni deposit.

3. Anodic process.- The aim of this second electrochemical process is to achieve higher solar absorption by coating the metal surface with an optical interference oxide layer. Thus we have to find adequate anodic conditions to promote the formation of a NiO film exhibiting a reproducible thickness of typically 0.1  $\mu\text{m}$  /13/.

3.1. Optimization of anodic conditions.- This part of our work has been greatly facilitated by an extensive study we made some years ago /14,15/ of anodic oxide films formed on nickel in concentrated sulfuric acid solutions. When a Ni anode is polarized in sulfuric acid concentrations up to about 4 N, one observes the formation of a passivating layer. But when the acid concentration is higher, there is an increase in anodic current showing that the electrode is no longer protected by the layer. Then the anode is covered with a stable oxide layer whose thickness depends on the electrochemical state of the system defined by anodic potential, acid concentration and temperature. The layer thickness is of course time dependent and tends towards a maximum /14/ which results from an equilibrium between a further oxidization of Ni at the Ni-NiO interface and a dissolution of NiO at the NiO-electrolyte interface /15/. Figure 5 gives the maximum thickness that can be obtained at 15°C for various acid media when the anodic potential changes from

500 mV up to 1000 mV/SCE. Slightly lower values have to be expected at room temperature /14/. What can be seen on these curves is the existence of a maximum for the oxide layer thickness in the medium potential range and, moreover, that the maximum thickness strongly depends on the sulfuric acid concentration.

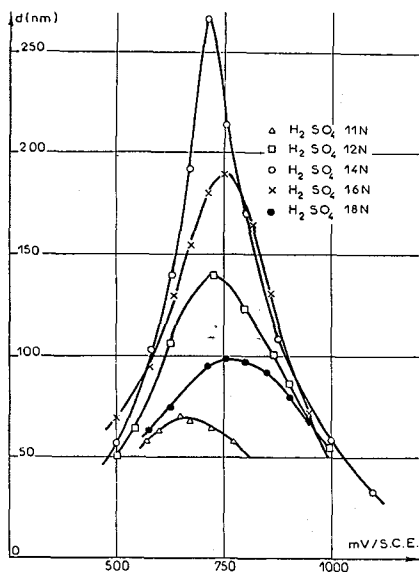


Fig.5.- Maximum thickness  $d$  of the oxide layer which can be formed on a Ni anode (at  $15^{\circ}\text{C}$ ) versus anodic potential for various sulfuric acid concentrations.

Thus we could start from a solution of 14 N  $\text{H}_2\text{SO}_4$ , which leads to the thickest oxide layer for an anodic potential of 725 mV/SCE, and switch off the cell once half the maximum thickness is reached. However it is not very convenient to operate in such a way, as a few seconds variation in the total duration of the anodic process would mean a great variation of thickness for the oxide layer. Since the growth kinetics for that oxide layer are of an exponential form /14/, it is far more secure to choose an acid concentration of 12 N which gives a maximum thickness slightly greater than the desired value and hence a safer latitude when interrupting the NiO growth process. Another advantage is that a lower concentration gives the oxide layer properties which are closer to bulk NiO /15/.

3.2. Optical properties of oxidized  $\langle 110 \rangle$  Ni deposits.- As for the cathodic process, the detailed electrochemical parameters were empirically chosen to optimize the reflectance curve. This was achieved in the following conditions : operating at room temperature ( $\sim 20^{\circ}\text{C}$ ) in a 12 N  $\text{H}_2\text{SO}_4$  solution, the anodic potential was potentiostatically controlled at 750 mV/SCE and the duration of the oxidization was 2 minutes.

Starting from a  $\langle 110 \rangle$  Ni electrodeposit as prepared according the procedure described in (2.2.), we then obtain a midnight blue sample whose typical reflectance is plotted in figure 6. As compared to figure 3, we do observe a decisive improvement and the more so for  $\lambda = 0.5$  to  $0.6 \mu\text{m}$  where the reflectance is only 1.5%.

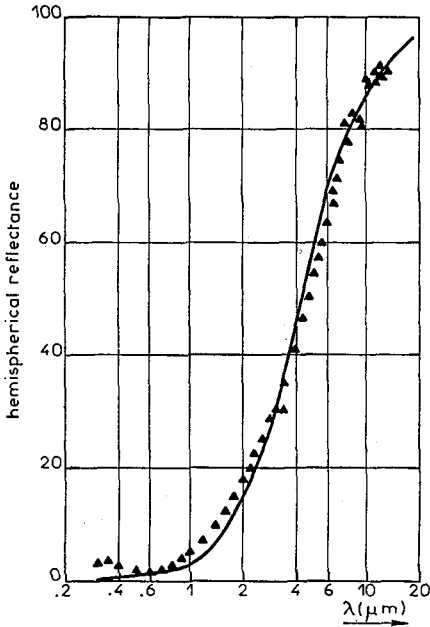


Fig.6.- Monochromatic hemispherical reflectance of an anodically-oxidized rough Ni deposit.  $\blacktriangle$  = optical measurements ; the solid line corresponds to Beckmann simulation.

Here again we have tried to account for such a curve with Beckmann's model. The best fit leads to computed values of :

$\sigma_1 = 0.20 \mu\text{m}$  ;  $T_1 = 0.05 \mu\text{m}$  and  $\sigma_2 = 0.64 \mu\text{m}$  ;  $T_2 = 0.20 \mu\text{m}$ , which must be compared to the values one can estimate from the micrographs of figure 7. If the amplitude of the low roughness seems to be realistic, it is no longer the case for the high roughness -whose amplitude has been underestimated- nor for both spatial periods which have been underestimated by a factor of 5 to 10.

If we now compare the micrographs of figures 4 and 7, it seems obvious that the anodic oxidization has not profoundly affected the initial rough structure of  $\langle 110 \rangle$  textured Ni. Such an observation is somewhat surprising, since the oxide formation is accompanied by a substantial dissolution of the underlying metal which could have severely modified the surface morphology. That the latter is preserved means that the Ni dissolution occurs according to a similar -although reverse- mechanism than for the growth. The solar absorptance  $\alpha$  and thermal emittance  $\varepsilon(T)$

computed from the results of figure 6 are listed in table II. It can be seen that the solar absorptance has considerably improved (up to 0.95) while the emittance has only been increased by a few percent.

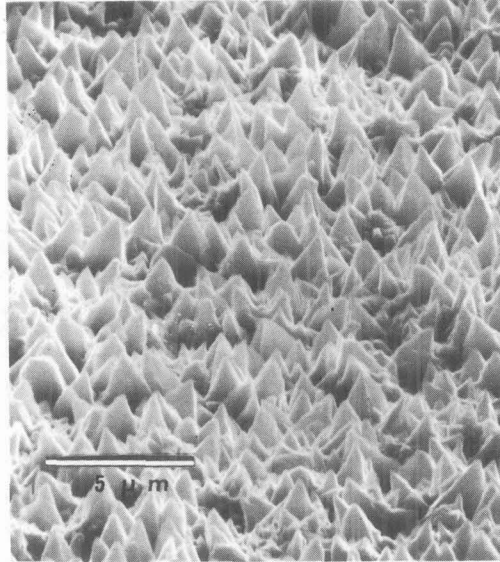


Fig.7a.-

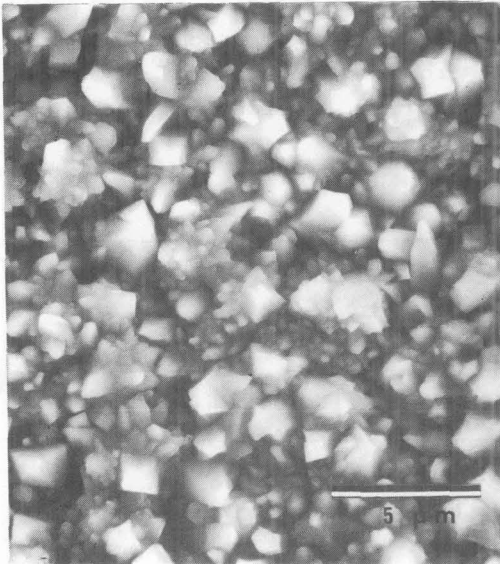


Fig.7b.-

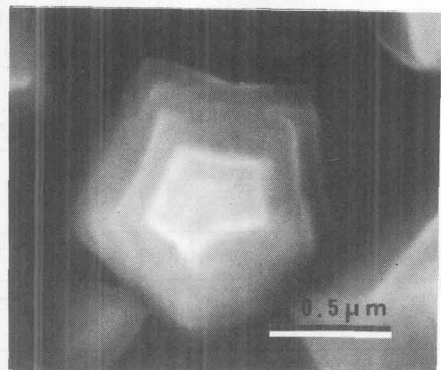


Fig.7c.-

Fig.7.- Scanning electron micrographs of the surface morphology of an oxidized Ni deposit after optimal anodic treatment. a/ grazing incidence, b/ top view, c/ detailed top view of a pentagonal pyramid.

ABSORPTANCE $\alpha$		EMITTANCE $\epsilon(T)$			
bright sun	clouded sun	30°C	100°C	200°C	300°C
0.953	0.944	0.12	0.16	0.23	0.30

Table II.- Selectivity parameters for an oxidized rough sample.

3.3. Thermal stability of oxidized samples.- Before assigning our samples to photothermal solar energy conversion, we must ensure that they are able to endure high temperatures for long periods without degradation. For that purpose we subjected most of them to progressive steps of thermal treatment, with a 20-hour maintenance at each step under air.

The data collected so far show no significant alteration of the optical properties, as measured by the variation of reflectance vs. wavelength, for treatments up to 300°C. A slight degradation begins to occur at 350°C, as can be seen from figure 8 where we plotted again the results of figures 3 and 6 for comparison. That after a 18-hour maintenance at 350°C the minimum of reflectance is shifted towards longer wavelengths probably means a thickening of the oxide layer due to a further thermal oxidization. Such a degradation results in a 3% decrease for the values of  $\alpha$  and  $\epsilon(T)$ , which are listed in table III, as compared to the values before thermal treatment. Experiments are now being carried on at higher temperatures to achieve a complete degradation in order to understand the structural reasons for it.

ABSORPTANCE $\alpha$		EMITTANCE $\epsilon(T)$			
bright sun	clouded sun	30°C	100°C	200°C	300°C
0.927	0.916	0.09	0.13	0.20	0.27

Table III.- Selectivity parameters after a 18-hour maintenance at 350°C of an anodically-oxidized rough sample.

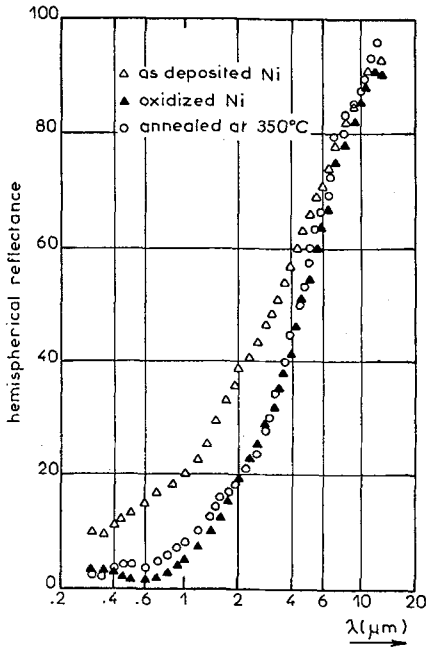


Fig.8.- Monochromatic hemispherical reflectance of an anodically-oxidized rough Ni sample after a 18-hour thermal treatment at 350°C in air. Experimental data of figures 3 and 6 are plotted again for comparison.

4. Conclusions.- Electrochemical processes, which are among the less-expensive surface treatments, are quite well-adapted to achieve high solar selectivity. One must never forget however that their results may be drastically altered by some variation of any among the numerous parameters which govern them. Hence, as a first requirement, good reproducibility will only be obtained through tight control of the whole set of parameters.

The major problem which must be solved subsequently is to determine which of these parameters are relevant to the expected optical properties. This paper shows how a long-term knowledge of the structural properties of rough Ni deposits may both direct the proper choice of plating conditions in order to optimize the solar absorptance and help to understand -thanks to the concept of texture- the morphological reasons accounting for wavelength discrimination.

In so far as the dendritic roughness responsible for short wavelength absorption is not modified by the further anodic treatment, the additional absorption provoked by the thin NiO layer merely stems from a destructive interference effect. Thus the whole process, which has just been patented /16/, gives a competitive method to prepare flat plate solar collectors for moderate temperatures applications, with both understandable and excellent selectivity properties.

References

- /1/ Tabor, H., Bull. Res. Council. of Israel 5A (1955) 119
- /2/ Pettit, R.B. and Sowell, R.R., J. Vac. Sci. Technol. 13 (1976) 596
- /3/ Froment, M. and Ostrowiecki, A Mét. Corr. Ind. 487 (1966) 83
- /4/ Epelboin, I., Froment, M. and Maurin, G., Plating 56 (1969) 1356
- /5/ Amblard, J., Froment, M. and Spyrellis, N., Surf. Technol. 5 (1977) 205
- /6/ Froment, M. and Maurin, G., J. Microsc. 7 (1968) 39
- /7/ Maurin, G., Oberfläche-Surface 11 (1970) 297, 309 ; 12 (1971) 8, 24
- /8/ Banerjee, B.C. and Goswami, A., J. Electrochem. Soc. 106 (1959) 20, 590
- /9/ Behaghel, J.M., Berthier, S., Lafait, J. and Rivory, J., Sol. Energy Mat. 1 (1979) 201
- /10/ Behaghel, J.M., Berthier, S., Lafait, J., J. Physique Colloq. 42 (1981) C1- this issue.
- /11/ Lafait, J., Behaghel, J.M., Berthier, S. and Rivory, J., J. Physique Colloq. 42 (1981) C1- this issue.
- /12/ Seraphin, B.O., in Solar Energy Conversion, Solid-State Physics Aspects, ed by B.O. Seraphin (Springer-Verlag) 1979 p.14
- /13/ Peterson, R.E. and Ramsey, J.W., J. Vac. Sci. Technol. 12 (1975) 174
- /14/ Blondeau, G., Froment, M. and Hugot-Le Goff, A., C.R. Hebd. Séan. Acad. Sci. Paris 271 C (1970) 795
- /15/ Blondeau, G., Froelicher, M., Froment, M. and Hugot-Le Goff A., Proc. Symp. on oxide-electrolyte interfaces, Miami Beach (1972), R. Alwitt ed, Electrochem. Soc. Inc., Princeton (1973) 215
- /16/ Blondeau, G., Amblard, J. and Froelicher, M., French Patent ANVAR n° 80.09959 (May 1980)